RSC Advances

PAPER

View Article Online
View Journal | View Issue

Cite this: *RSC Adv.*, 2026, **16**, 23005

Magneto-electrochemical approach for determining the rate-controlling step for corrosion of iron in ferric solutions

Haiying Dong,[ab] Fujie Zhou,[ab] Xiujie Wang,[ab] Zhanpeng Lu,[*abc] Tongming Cui,[*ab] Xin Li,[ab] Juan Wang,[ab] Xinhe Xu,[ab] Junjie Chen[ab] and Tetsuo Shoji[d]

Received 25th February 2026
Accepted 17th April 2026

DOI: 10.1039/d6ra01642a

rsc.li/rsc-advances

The rate-controlling step for the corrosion of iron in ferric solutions is determined by electrochemical measurements under a magnetic field. A positive shift in open circuit potential and the increase of cathodic current by imposing a magnetic field indicate that the contribution of the mass transport process of reactive species to rate control. The corrosion rate of iron under open circuit conditions is controlled by both the mass transport step and the electron transfer step. There is a potential region in which the ferric reduction rate is fully controlled by the mass transport process, as indicated by the potential independence of the resulting current density from the magnetic field.

1. Introduction

Corrosion is the chemical degradation of materials, such as metals, semiconductors, insulators, and even polymers, due to exposure to the environment.[1] Depending on the combinations of materials and environments, there are various electrochemical processes involved in corrosion, leading to different types of rate-controlling steps (RCSs) for corrosion reactions.[2–4] The rate-controlling step can be an electron-transfer step (ETS), mass-transport step (MTS), or mixed type involving both ETS and MTS. The rate-controlling step can arise from anodic reaction, cathodic reaction, or both. Determining the RCS is critical for understanding corrosion mechanisms and reaction kinetics, as well as the way to mitigate corrosion. Direct current (DC) electrochemical measurements, such as potentiostatic polarization and potentiodynamic polarization curves,[5,6] and alternative current measurements, such as electrochemical impedance spectroscopy (EIS), have been used to determine the rate-controlling step for corrosion reactions.[7–10] DC measurements are sometimes lacking information for the open circuit state conditions. EIS is often used for determining the RCS under open circuit states, but it needs noise-prevention and professional analytical interpretation.[5]

Based on available data interrelated to the magnetic field (MF) effects on electrochemical behavior, in many cases, steady state MFs would affect the MTS for reactive charge-bearing species[11–21] but do not have any significant effect on ETS.[15,22–27] The effect of MF on the electrochemical system is mainly attributed to the influence of additional forces introduced by MF on the ions in the electrolyte. The additional forces, including Lorentz force, magnetic field gradient force, paramagnetic force, magnetic damping force and electrokinetic shear stress, have been interpreted.[28] Among them, magnetohydrodynamic (MHD) effect and magnetic field gradient force effect (MFGF) are generally accepted to interpret the MF effect on the electrochemical reaction of metals in corrosive solutions. The MHD effect involving the interaction of the MF with the local electric current density is driven by the Lorentz force acting on the moving charge. This effect accelerates the convection of the electrolyte, enhances the mass transfer significantly and reduces the thickness of the diffusion layer.[11,13,17,18,27–34] The limiting current in the regime controlled by mass transport increases due to the localized stirring of the electrolyte resulting from MF. The amplitude and direction of the Lorentz force are related to the relative direction of the MF and electrode surface, such as being parallel or perpendicular to each other. The consequence of the Lorentz force increases with magnetic field intensity, varying as $B^{1/3}$.[30] MFGF effect driven by magnetic field gradient force, and it is only important for convection of the electrolyte when nonhomogeneous MF are present and could overcome the impact of the Lorentz force. It directly applies to the paramagnetic substances in the electrolyte and pulls paramagnetic or diamagnetic substances into or away from the high magnetic flux density areas on the electrode surface, so as to accelerate the cathodic reaction or inhibit the anodic dissolution.[28,35] MF only influences the anodic dissolution, partly or fully controlled by the mass transfer step, but has no impact on the fully controlled by electron transfer step.[11,13,18,20] Based on these observations, a novel approach

[a]*State Key Laboratory of Materials for Advanced Nuclear Energy, Shanghai University, Shanghai, 200444, China. E-mail: zplu@t.shu.edu.cn; cuitongming@shu.edu.cn*
[b]*School of Materials Science and Engineering, Shanghai University, Shanghai 200444, China*
[c]*Jiangsu Yihai New Energy Material Sci. and Tech., Co. Ltd, Jiangsu, 214233, China*
[d]*New Industry Creation Hatchery Center, Tohoku University, Sendai, 980-8579, Japan*

based on electrochemical measurements under MF effects, called the magneto-electrochemical method, is proposed for determining the RCS for corrosion reactions. Systems with iron in ferric ion solutions are used in the present research.

2. Experimental material and method

The experimental material is industrial iron of 99.5% purity. Electrochemical measurement, including potentiostatic polarization and the open circuit potential OCP, and weight loss tests were conducted to complete this work. The all-electrochemical tests were conducted by the electrochemical workstation Gamry ref. 1010 Potentiostat/Galvanostat/ZRA controlled by PC. The electrochemical experimental device and the preparation for the three electrodes are similar to those in the papers previously published by the research group.[24–26] The electrolytic solutions were x mol L^{-1} $Fe_2(SO_4)_3$ solution ($x = 0.02$, 0.05, 0.1, 0.2) prepared with $Fe_2(SO_4)_3$ of analytical pure grade and high purity water, which were used as the sources of ferric ions to investigate the effect of MF on typical cathodic reactions. In this work, applying different intensity MF (0 T, 0.05 T, 0.1 T, 0.2 T, 0.3 T, 0.4 T and 0.5 T) generated by the P5 model electromagnet power supply on both sides of the electrolytic cell. The pure iron is situated in the center of the two iron cores. The MF direction is parallel to the working face of pure iron.

The shift of OCP after applying or withdrawing the MF, $\Delta E_{corr,MF}$, was used as one of the key parameters for determining the RCS for corrosion systems.[15] The OCP of the working electrode would become stable after immersing in an electrochemical cell for a period of time under 0T, recording as E_{corr}. Then the MF was quickly applied from 0.05 T to 0.5 T by several steps. The OCP under MF was recorded as $E_{corr,MF}$ and needed to reach a stable state under each magnetic field intensity. Subsequently, the MF was withdrawn from 0.5 T to 0 T by several steps. The $\Delta E_{corr,MF}$ was calculated with eqn (1),

$$\Delta E_{corr,MF} = E_{corr,MF} - E_{corr} \quad (1)$$

The change of current density obtained by potentiostatic polarization in response to the application of MFs was used as another parameter for determining RCS at specific potentials. The procedures are shown below. When an electrode was polarized at potential E in the test solutions and the current density reached the steady state, recording the current density as $i(E)$, then the MF was applied on the working electrode and the current density at the steady state as $i^*(E)$. The change of the current density resulting from MF, $\Delta i_{MF}(E)$, can be calculated by eqn (2). According to the $\Delta i_{MF}(E)$. The RCS for the electrode reaction at a certain potential can be determined. For example, if $\Delta i_{MF}(E)$ did not change with E in a specific potential range, MTS was thought to be the RCS for this electrode reaction in this potential range. The potentiostatic polarization was conducted with several steps, including applying or withdrawing MF. The electrode was at first potentiostatically polarized at a selected potential E for 400 s under 0T, then the MF was quickly applied and held constant for 400 s, and then the MF was quickly withdrawn. These steps were repeated. Current density was monitored during the whole test period.

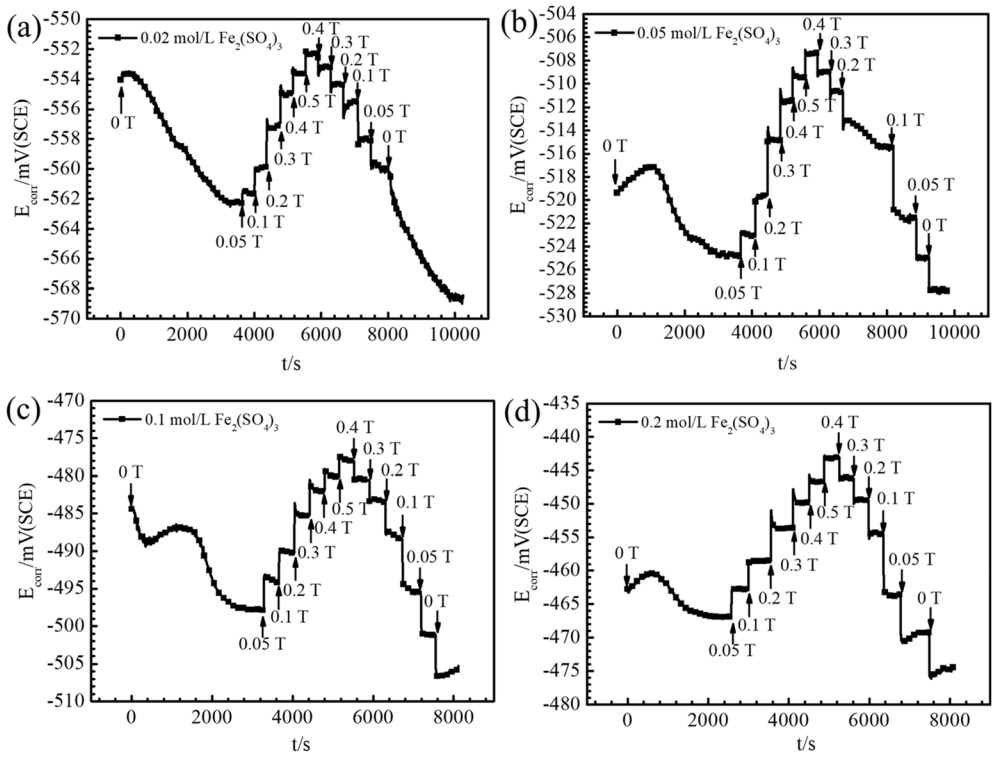

Fig. 1 Response of E_{corr} to applying or withdrawing the magnetic field curve for Fe in x mol L^{-1} $Fe_2(SO_4)_3$ solutions. (a) $x = 0.02$; (b) $x = 0.05$; (c) $x = 0.1$; (d) $x = 0.2$.

$$\Delta i_{MF}(E) = i^*(E) - i(E) \quad (2)$$

Cathodic polarization curves by potentiodynamic sweep with MF ON-OFF were measured in ferric-free sulfuric acid solutions with the same pH values as those for ferric ion solutions, *i.e.*, 0.0039 mol L^{-1} H_2SO_4 solution with the same measured pH values of 2.11 for 0.02 mol L^{-1} $Fe_2(SO_4)_3$ solution, 0.0087 mol L^{-1} H_2SO_4 solution with the same measured pH values of 1.76 for 0.05 mol L^{-1} $Fe_2(SO_4)_3$ solution, 0.0160 mol L^{-1} H_2SO_4 solution with the same measured pH values of 1.52 for 0.10 mol L^{-1} $Fe_2(SO_4)_3$ solution, and 0.0295 mol L^{-1} H_2SO_4 solution with the same measured pH values of 1.23 for 0.20 mol L^{-1} $Fe_2(SO_4)_3$ solution. These tests were designed to distinguish the response of the current density from ferric reduction or hydrogen ion reduction to the magnetic field.

Weight loss tests were performed under both 0 T and 0.4 T at room temperatures of about 25 °C. The samples for weight loss tests were 60 mm × 20 mm × 3 mm. The sample surfaces were ground up to 1500-grit abrasive paper, rinsed with ethanol and acetone, and then dried with cold air before the tests. The samples were immersed in $Fe_2(SO_4)_3$ solutions for 1.0 h. The weights of the samples were measured before and after the immersion tests. The average corrosion rate was calculated based on the change of the specimen weight, the surface area (S), and the immersion time (t), according to eqn (3). In this weight loss test, four parallel samples are prepared for each experimental condition to ensure the accuracy of the data.

$$CR = \frac{W_0 - W_1}{S \times t} \quad (3)$$

3. Results

3.1 The shift of open circuit potential resulting from the magnetic field

The responses of E_{corr} for iron in $Fe_2(SO_4)_3$ solutions to imposing or withdrawing MF are shown in Fig. 1 and 2. E_{corr} shifted in the positive direction after applying MF, and the magnitude of the E_{corr} shift increased with increasing B from 0 T to 0.5 T. E_{corr} shifted in the negative direction after decreasing the B step by step from 0.5 T to 0 T. The memory effect due to MF on OCP was not significant. The values of E_{corr} would not be the same under similar conditions, which might arise from the slight change of the surface roughness of the working electrode after immersing in corrosive test solutions for a relatively long time. The value of $\Delta E_{corr,MF}$ increased with increasing B as well as increasing the ferric ions concentration, as shown in Fig. 3.

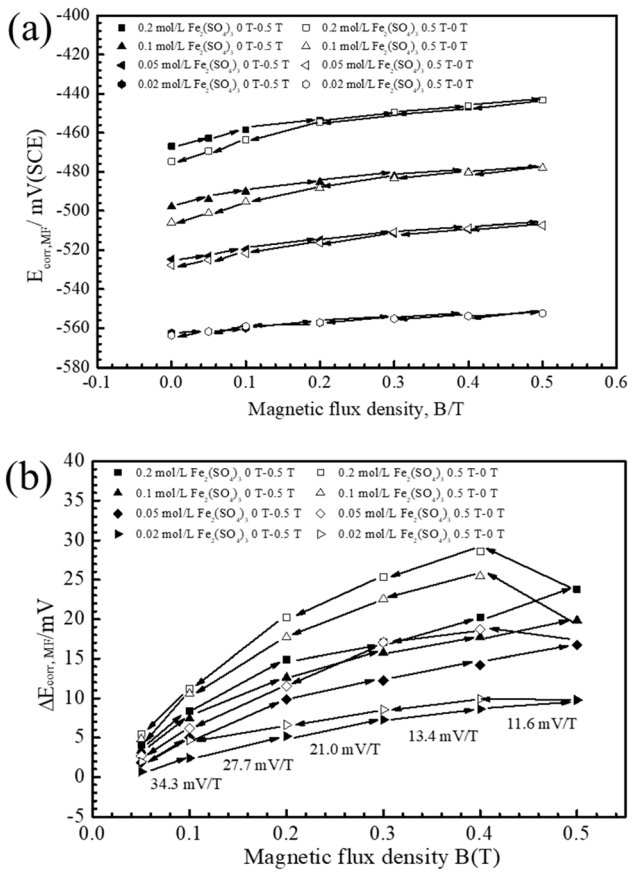

Fig. 2 The open circuit potentials for Fe in $Fe_2(SO_4)_3$ solutions in the absence or presence of a magnetic field. (a) E_{corr} vs. B; (b) $\Delta E_{corr,MF}$ *vs.* B.

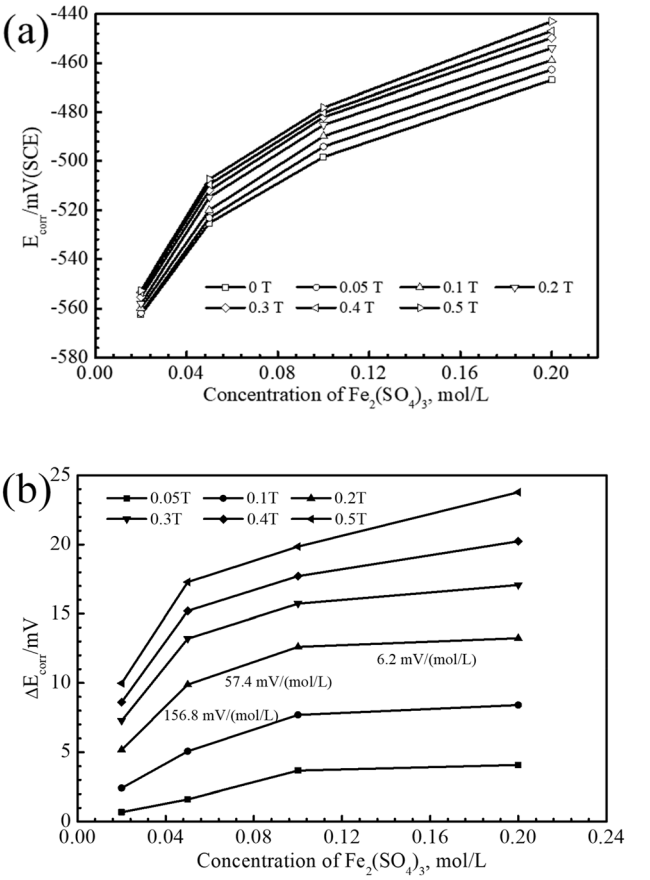

Fig. 3 The open circuit potentials for Fe in $Fe_2(SO_4)_3$ solutions in the absence or presence of a magnetic field. (a) E_{corr} vs. concentration of $Fe_2(SO_4)_3$; (b) $\Delta E_{corr,MF}$ *vs.* $Fe_2(SO_4)_3$ concentration.

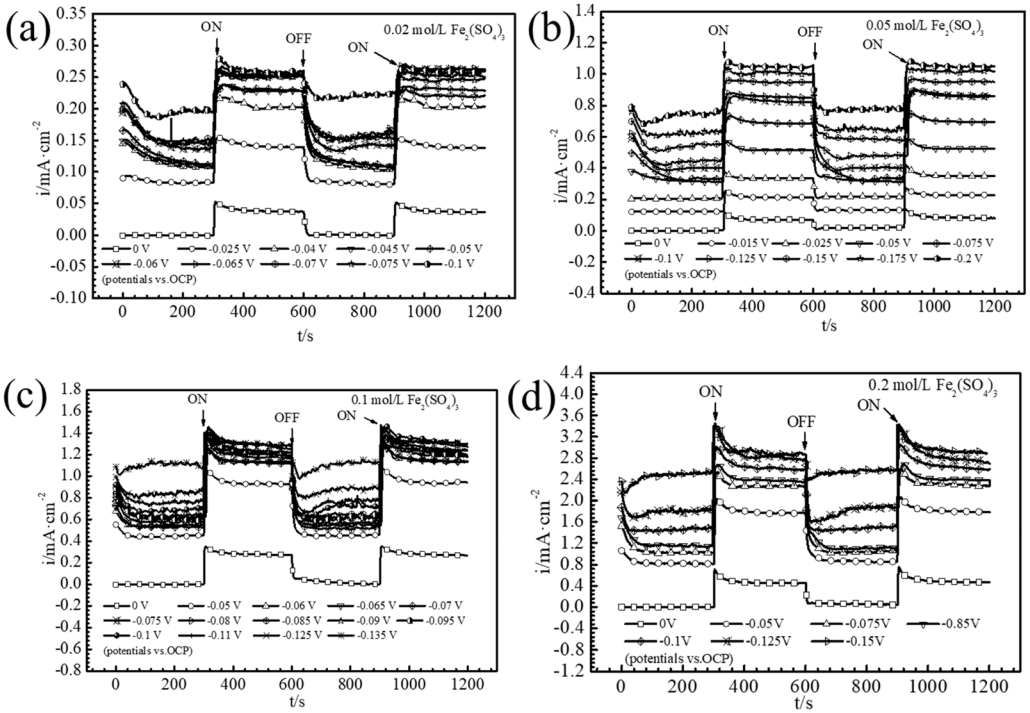

Fig. 4 Cathodic current density–time curve for Fe in x mol L^{-1} $Fe_2(SO_4)_3$ solutions with 0T or 0.4 T magnetic field at various potentials. (a) $x = 0.02$; (b) $x = 0.05$; (c) $x = 0.1$; (d) $x = 0.2$.

3.2 The change of current density resulting from the magnetic field

Current densities for iron in $Fe_2(SO_4)_3$ solutions at various potentials under 0 T or 0.4 T MF are summarized in Fig. 4. The changes of current density resulting from MF with 0.4 T, $\Delta i_{0.4T}(E)$, are calculated with eqn (2) and the results are shown in Fig. 5. At all these potentials, the cathodic current density became higher after applying MF, and became lower after withdrawing MF. With the negative shift of potential E, the bubbles in the solution

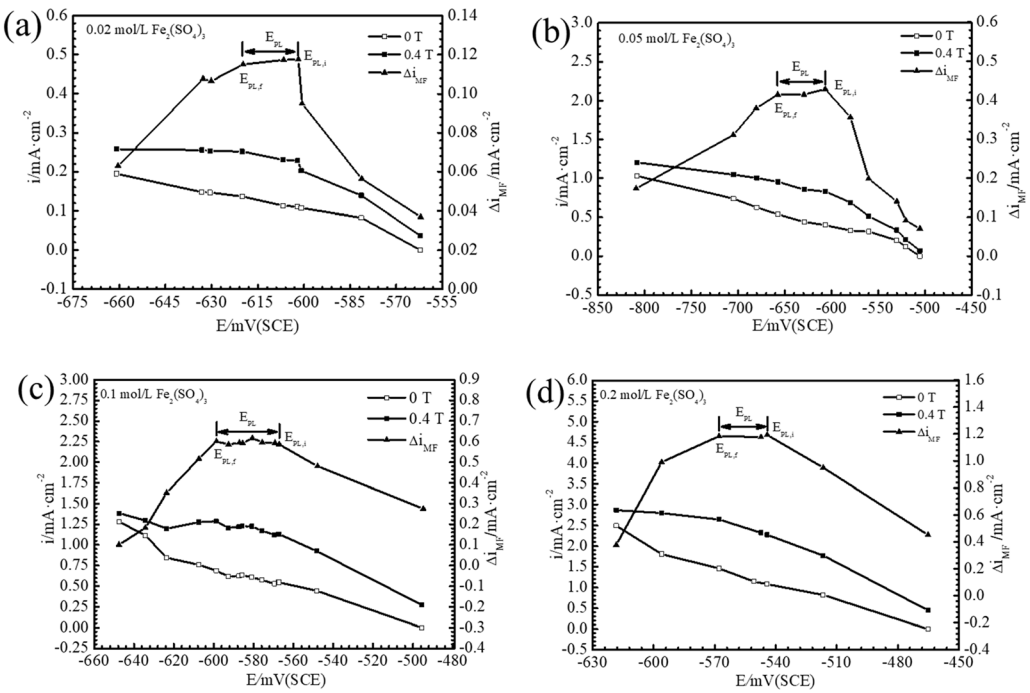

Fig. 5 Cathodic current density (i) or the changes of cathodic current density (Δi_{MF}) resulted from the magnetic field at various potentials (E) for Fe in x mol L^{-1} $Fe_2(SO_4)_3$ solutions. (a) $x = 0.02$; (b) $x = 0.05$; (c) $x = 0.1$; (d) $x = 0.2$.

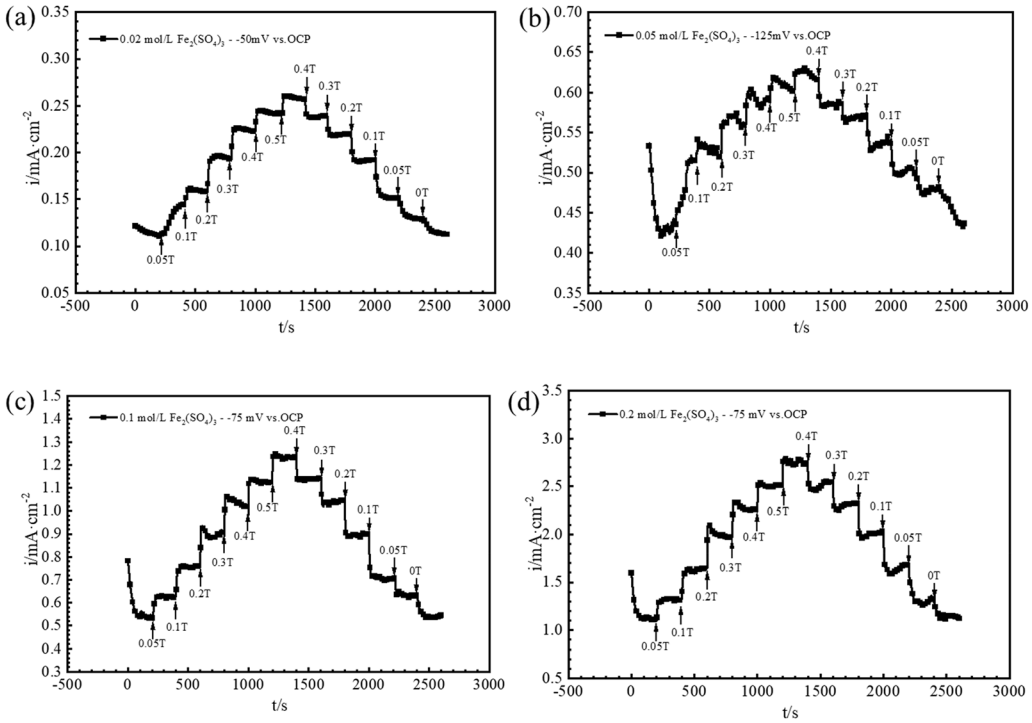

Fig. 6 Current density after applying or withdrawing a magnetic field at potential E that is in the E_{PL} potential range for Fe in x mol L^{-1} $Fe_2(SO_4)_3$ solutions. (a) $x = 0.02$, $E = -50$ mV_{OCP}; (b) $x = 0.05$, $E = -125$ mV_{OCP}; (c) $x = 0.1$, $E = -75$ mV_{OCP}; (d) $x = 0.2$, $E = -75$ mV_{OCP}.

increased, and the hydrogen evolution reaction became more important. $\Delta i_{0.4\ T}(E)$ at first increased with decreasing applied potential and then reached a quasi-plateau in the potential range between $E_{PL,i}$ and $E_{PL,f}$. In this potential range marked as E_{PL}, $\Delta i_{0.4\ T}(E)$ is insensitive or independent of potential. $\Delta i_{0.4T}(E)$ decreased with decreasing potential if the potential was more negative than $E_{PL,f}$ or more positive than $E_{PL,i}$.

Based on the measured cathodic polarization curves, −150 mV_{OCP}, −125 mV_{OCP}, −75 mV_{OCP} and −75 mV_{OCP} for Fe in 0.02, 0.05, 0.1 and 0.2 mol L^{-1} $Fe_2(SO_4)_3$ solutions were chosen for cathodically potentiostatic polarization under MFs. Those potentials were located in the potential range where $\Delta i_{MF}(E)$ was nearly independent of potential E. The values of cathodic current density for Fe in $Fe_2(SO_4)_3$ solutions were summarized in Fig. 6. The cathodic current density increased with increasing B. After withdrawing the MF step by step, the current density can roughly return to its original value obtained under the same magnetic field before withdrawing the MF. The current density increased or decreased rapidly in the initial stage after applying or withdrawing MF, then reached a stable value during prolonged polarization. Under the same B, the cathodic current density increased with increasing ferric ion concentration. The values of $\Delta i_{MF}(E)$ are shown in Fig. 7, indicating that the effect of the MF on current density increased with increasing B or increasing ferric concentration.

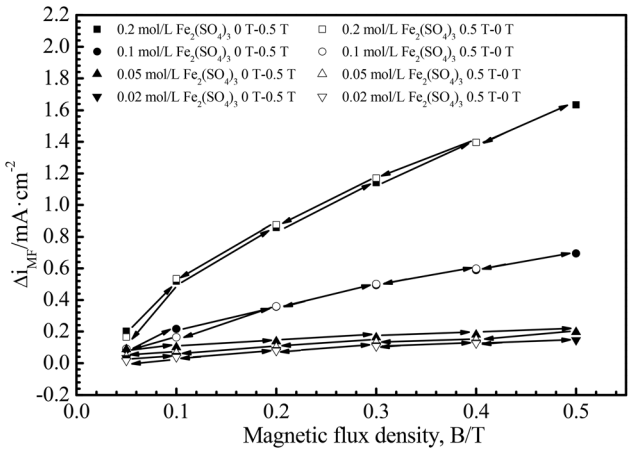

Fig. 7 Current density resulting from the magnetic field at polarization potential −50 mV_{OCP}, −125 mV_{OCP}, −75 mV_{OCP} and −75 mV_{OCP} that is in the E_{PL} potential range for Fe in 0.02 mol L^{-1}, 0.05 mol L^{-1}, 0.1 mol L^{-1}, and 0.2 mol L^{-1} $Fe_2(SO_4)_3$ solutions.

3.3 Cathodic polarization curves in sulfuric acid solutions

The results in Fig. 8 showed that during the potentiodynamic polarization for Fe in several H_2SO_4 solutions, the current density did not exhibit a significant change after applying a 0.4 T MF pulse, which was similar after withdrawing MF. These results indicated that the effect of MF on hydrogen reduction was less significant than that on ferric reduction. The change of the current density as a result of applying or withdrawing MF for iron in ferric solution was thought to be mainly due to the effect of MF on ferric ion reduction, as shown in Fig. 4 and 6, which was also applicable to the shift of OCP under multiple magnetic field intensities, as shown in Fig. 1.

3.4 Corrosion rates under 0 T and 0.4 T

Fig. 9 shows the average corrosion rates for Fe in $Fe_2(SO_4)_3$ solutions in the absence or presence of MF and the ratios of

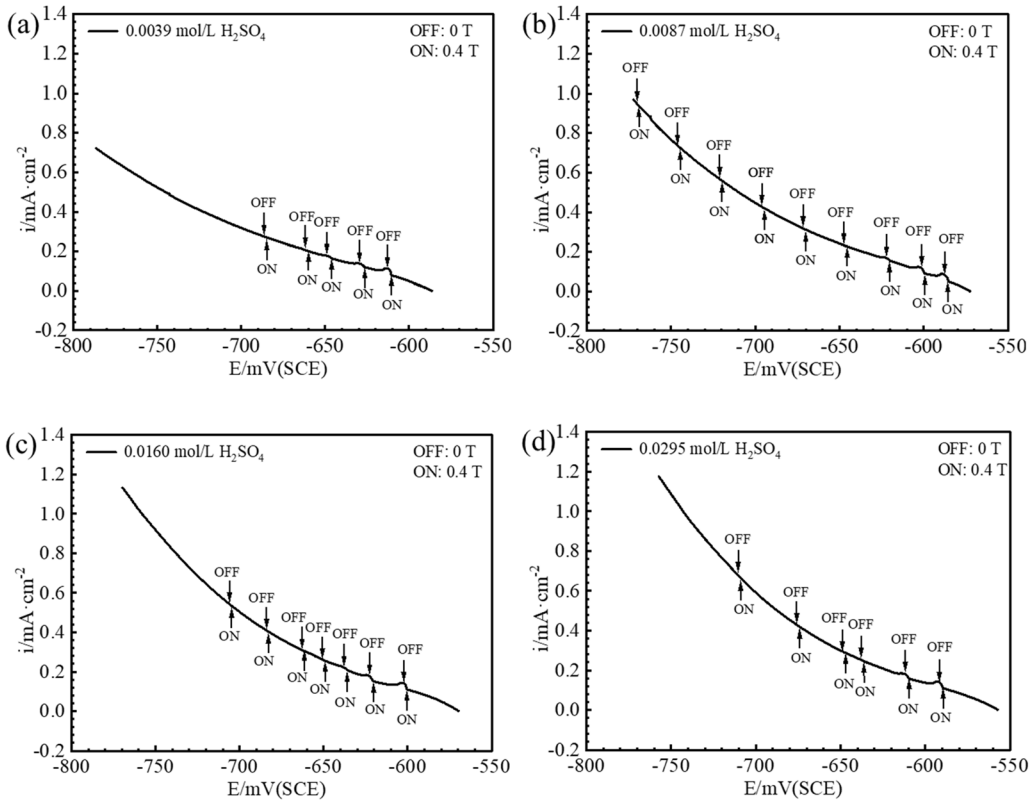

Fig. 8 Cathodic polarization curve for Fe in H_2SO_4 solutions. (a) 0.0039 mol L^{-1} H_2SO_4; (b) 0.0087 mol L^{-1} H_2SO_4; (c) 0.0160 mol L^{-1} H_2SO_4; (d) 0.0295mol L^{-1} H_2SO_4.

$CR_{0.4T}/CR_{0T}$. The corrosion rate was higher under 0.4 T than that under 0 T, indicating that MF would accelerate corrosion under OCP conditions. Corrosion rate increased with the increase of ferric concentration under 0 T or 0.4 T. The $CR_{0.4T}/CR_{0T}$ ratio increased with the increase of the ferric concentration, indicating that the effect of MF on the cathodic current density increased with the increase of ferric concentration.

4. Discussion

Magneto-electrochemical measurements are designed and used in the present work as a new approach for determining the rate-controlling step(s) for corrosion reactions. The $\Delta E_{corr,MF}$ as well as the $\Delta i_{MF}(E)$ under potentiostatic polarization, as the response to applying or withdrawing MF, is used as a criterion for judging the RCS. In all cases, it is assumed that MF changes only the rate of the reactions but not the type of the reactions. $\delta_{MF}(E)$ is used as the modulation factor by MF on current density at potential E, which is related to the types of reactions and their corresponding RCS. $\delta_{MF}(E)$ is represented by $\delta_{MF,L,Fe^{3+}}(E)$ on diffusion of ferric ions from the electrode to the solution, by $\delta_{MF,Fe^{3+}/Fe^{2+}}(E)$ on charge transfer of ferric reduction, and by $\delta_{MF,H^+/H_2}(E)$ on proton reduction, respectively.

$$i^*(E) = \delta_{MF} \cdot i(E) \quad (4)$$

$$i^*(E) = i_a^*(E) + i_c^*(E) \quad (5)$$

$$i_a^*(E) = \delta_{MF,a} \cdot i_a(E) \quad (6)$$

$$i_c^*(E) = \delta_{MF,c} \cdot i_c(E) \quad (7)$$

Taking the active dissolution of iron controlled by ETS as the dominant anodic reaction at potential E near E_{corr}, combining eqn (6) and (A10),

$$i_a^*(E) = \delta_{MF,a} \cdot i_{0,Fe/Fe^{2+}} \cdot e^{\frac{E - E_{e,a,Fe/Fe^{2+}}}{\beta_{a,Fe/Fe^{2+}}}} \quad (8)$$

There are mainly two cathodic reactions at potentials near E_{corr}, *i.e.*, ferric reduction and proton reduction.

$$i^*_{c,Fe^{3+}/Fe^{2+}}(E) = \delta_{MF,c,Fe^{3+}/Fe^{2+}} \cdot i_{c,Fe^{3+}/Fe^{2+}}(E) \quad (9)$$

$$i^*_{c,H^+/H_2}(E) = \delta_{MF,c,H^+/H_2} \cdot i_{c,H^+/H_2}(E) \quad (10)$$

Taking ETS as the RCS for proton reduction, combining eqn (10) and (A11),

$$i^*_{c,H^+/H_2}(E) = \delta_{MF,c,H^+/H_2} \cdot i_{0,H^+/H_2} \cdot e^{\frac{E_{e,c,H^+/H_2} - E}{\beta_{c,H^+/H_2}}} \quad (11)$$

If tentatively taking both ETS and MTS as RCSs for ferric reduction, combining eqn (9) and (A12),

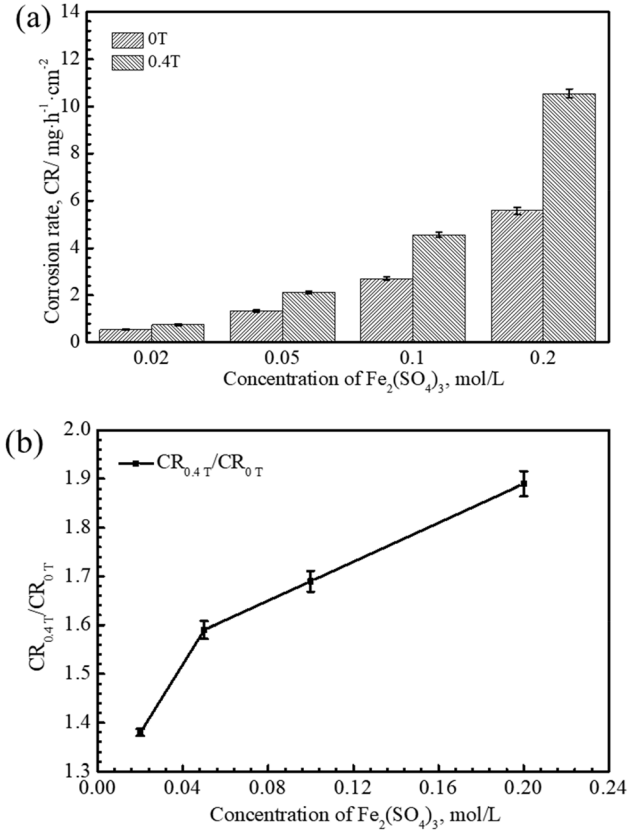

Fig. 9 (a) Corrosion rates of iron in $Fe_2(SO_4)_3$ solutions under 0 T and 0.4 T; (b) $CR_{0.4T}/CR_{0T}$ *vs.* concentration of $Fe_2(SO_4)_3$.

$$i^*_{c,Fe^{3+}/Fe^{2+}}(E) = \delta_{MF,c,Fe^{3+}/Fe^{2+}} \cdot \frac{i_{0,Fe^{3+}/Fe^{2+}} \cdot e^{\frac{E_{e.c,Fe^{3+}/Fe^{2+}} - E}{\beta_{c,Fe^{3+}/Fe^{2+}}}}}{1 + \frac{i_{0,Fe^{3+}/Fe^{2+}} \cdot e^{\frac{E_{e.c,Fe^{3+}/Fe^{2+}} - E}{\beta_{c,Fe^{3+}/Fe^{2+}}}}}{i_{L,Fe^{3+}}}} \quad (12)$$

Based on the literature data on the effect of MFs on electrochemical reactions, it has been acknowledged that MF affects primarily the MTS of charge-bearing reactive species but not the ETS. Some exceptional cases have been reported for the possibility of the MF effects on charge-transfer controlled reactions such as proton reduction or anodic dissolution of iron.[36–38] For facilitating the discussion of the primary points of view, it is assumed that the effect of MF on ETS is negligible in the present research, which can be partly supported by the results in Fig. 8. There are,

$$\delta_{MF,a} = 1 \quad (13)$$

$$i^*_a(E) = i_{0,Fe/Fe^{2+}} \cdot e^{\frac{E - E_{e.a,Fe/Fe^{2+}}}{\beta_{a,Fe/Fe^{2+}}}} \quad (14)$$

$$\delta_{MF,c,H^+/H_2} = 1 \quad (15)$$

$$i^*_{c,H^+/H_2}(E) = i_{0,H^+/H_2} \cdot e^{\frac{E_{e.c,H^+/H_2} - E}{\beta_{c,H^+/H_2}}} \quad (16)$$

$$\delta_{MF,c,Fe^{3+}/Fe^{2+}}(E) = \frac{1 + \frac{i_{0,Fe^{3+}/Fe^{2+}} \cdot e^{\frac{E_{e.c,Fe^{3+}/Fe^{2+}} - E}{\beta_{c,Fe^{3+}/Fe^{2+}}}}}{i_{L,Fe^{3+}}}}{1 + \frac{i_{0,Fe^{3+}/Fe^{2+}} \cdot e^{\frac{E_{e.c,Fe^{3+}/Fe^{2+}} - E}{\beta_{c,Fe^{3+}/Fe^{2+}}}}}{i^*_{L,Fe^{3+}}}} \quad (17)$$

$$i^*(E) = \frac{i_{0,Fe^{3+}/Fe^{2+}} \cdot e^{\frac{E_{e.c,Fe^{3+}/Fe^{2+}} - E}{\beta_{c,Fe/Fe^{2+}}}}}{1 + \frac{i_{0,Fe^{3+}/Fe^{2+}} \cdot e^{\frac{E_{e.c,Fe^{3+}/Fe^{2+}} - E}{\beta_{c,Fe^{3+}/Fe^{2+}}}}}{i^*_{L,Fe^{3+}}}} + i_{0,H^+/H_2} \cdot e^{\frac{E_{e.c,H^+/H_2} - E}{\beta_{c,H^+/H_2}}} - i_{0,Fe^{3+}/Fe^{2+}} \cdot e^{\frac{E - E_{e.a,Fe^{3+}/Fe^{2+}}}{\beta_{a,Fe/Fe^{2+}}}} \quad (18)$$

It has been reported that diffusion of reactive charged species is related to the magnetohydrodynamics (MHD) effect[28–35,39–41] and magnetic field gradient force (MFGF) effect[42,43] driven by Lorentz-force and Kelvin-force-driven, respectively. The effect of the horizontal MF parallel to the working electrode surface on the mass transport rate at the metal/solution interface is attributed to the MHD effect. The total force, F, applied to the moving charged particle can be expressed by eqn 19–21.[26,41] The moving charged particle with the velocity of V_0 can be affected by MF, leading to a change in cathodic diffusion current density. The total velocity of a moving charged particle, $\boldsymbol{V}_{MF}$, includes $\boldsymbol{V}_0$ as well as $\boldsymbol{V}_{MHD}$ resulted from the magnetic field, can be expressed by eqn (22). $\boldsymbol{F}_{MHD}$ and $\boldsymbol{V}_{MHD}$ increase with increasing B, corresponding to the change of flux density J and current density i, eqn (23) and (24).

$$\boldsymbol{F} = \boldsymbol{F}_E + \boldsymbol{F}_{MHD} \quad (19)$$

$$\boldsymbol{F}_E = q\boldsymbol{E} \quad (20)$$

$$\boldsymbol{F}_{MHD} = \boldsymbol{J} \times \boldsymbol{B} \quad (21)$$

$$\boldsymbol{V}_{MF} = \boldsymbol{V}_{0T} + \boldsymbol{V}_{MHD} \quad (22)$$

$$\boldsymbol{J}_{MF} = \boldsymbol{J}^* = \boldsymbol{J}_{0T} + \boldsymbol{J}_{MHD} \quad (23)$$

$$\boldsymbol{i}_{MF} = \boldsymbol{i}^* = \boldsymbol{i}_{0T} + \boldsymbol{i}_{MHD} \quad (24)$$

For the diffusion of ferric ions from the bulk test solution to the iron electrode under MF, the limiting diffusion current density can be expressed by eqn (25).

$$\boldsymbol{i}^*_{L,Fe^{3+}} = \boldsymbol{i}_{L,Fe^{3+}} + \boldsymbol{i}_{MHD,Fe^{3+}} \quad (25)$$

For the MF perpendicular to the current direction, there is,

$$\boldsymbol{i}^*_{L,Fe^{3+}} > \boldsymbol{i}_{L,Fe^{3+}} \quad (26)$$

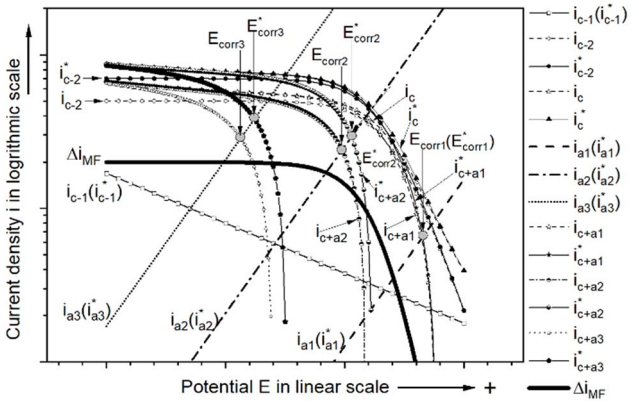

Fig. 10 Schematic of the effect of the magnetic field on corrosion processes based on electrochemical kinetics represented by the Evans diagram.

Based on the electrochemical kinetics equations in Appendix A1 and eqn 1–26 as well as the concept of the Evans diagram for corrosion reactions,[1,5,15,44,45] the effects of MF on the electrochemical behaviors of metal in corrosive solutions can be schematically shown in Fig. 10. A similar schematic diagram has been proposed in previous publications, where only one cathodic reaction is considered. The following discussion is based on the concept shown in Fig. 10 with six cathodic polarization curves, considering two cathodic reactions and one anodic reaction. Cathodic reaction c-1 is taken to be controlled by ETS, cathodic reaction c-2 is taken to be controlled by mixed ETS and MTS, and anodic reaction is taken to be controlled by ETS. Depending on the magnitude of the anodic reaction rate, as indicated by the curves i_{a1} (i^*_{a1}), i_{a2} (i^*_{a2}) and i_{a3} (i^*_{a3}) in Fig. 10, the OCP as the point of intersection of the true anodic and cathodic polarization curves, can be achieved at different potential values with different RCSs. The values of the difference between the polarization curve under MF and that under 0T, Δi_{MF}, are calculated and shown in Fig. 10.

4.1 Correlating open circuit potential to RCS

At open circuit potential under 0T, there is

$$i(E_{corr}) = 0 \tag{27}$$

$$\frac{i_{0,Fe^{3+}/Fe^{2+}} \cdot e^{\frac{E_{e.c,Fe^{3+}/Fe^{2+}} - E_{corr}}{\beta_{c,Fe^{3+}/Fe^{2+}}}}}{1 + \frac{i_{0,Fe^{3+}/Fe^{2+}} \cdot e^{\frac{E_{e.c,Fe^{3+}/Fe^{2+}} - E_{corr}}{\beta_{c,Fe^{3+}/Fe^{2+}}}}}{i_{L,Fe^{3+}}}} + i_{0,H^+/H_2} \cdot e^{\frac{E_{e.c,H^+/H_2} - E_{corr}}{\beta_{c,H^+/H_2}}}$$

$$- i_{0,Fe^{3+}/Fe^{2+}} \cdot e^{\frac{E_{corr} - E_{e.a,Fe^{3+}/Fe^{2+}}}{\beta_{a,Fe^{3+}/Fe^{2+}}}} = 0 \tag{28}$$

At open circuit potential under MF, there is

$$i^*(E^*_{corr}) = 0 \tag{29}$$

$$\frac{i_{0,Fe^{3+}/Fe^{2+}} \cdot e^{\frac{E_{e.c,Fe^{3+}/Fe^{2+}} - E^*_{corr}}{\beta_{c,Fe/Fe^{2+}}}}}{1 + \frac{i_{0,Fe^{3+}/Fe^{2+}} \cdot e^{\frac{E_{e.c,Fe^{3+}/Fe^{2+}} - E^*_{corr}}{\beta_{c,Fe^{3+}/Fe^{2+}}}}}{i^*_{L,Fe^{3+}}}} + i_{0,H^+/H_2} \cdot e^{\frac{E_{e.c,H^+/H_2} - E^*_{corr}}{\beta_{c,H^+/H_2}}}$$

$$- i_{0,Fe/Fe^{2+}} \cdot e^{\frac{E^*_{corr} - E_{e.a,Fe/Fe^{2+}}}{\beta_{a,Fe/Fe^{2+}}}} = 0 \tag{30}$$

Combining eqn (28) and (30),

$$\frac{i_{0,Fe^{3+}/Fe^{2+}} \cdot e^{\frac{E_{e.c,Fe^{3+}/Fe^{2+}} - E_{corr}}{\beta_{c,Fe^{3+}/Fe^{2+}}}}}{1 + \frac{i_{0,Fe^{3+}/Fe^{2+}} \cdot e^{\frac{E_{e.c,Fe^{3+}/Fe^{2+}} - E_{corr}}{\beta_{c,Fe^{3+}/Fe^{2+}}}}}{i_{L,Fe^{3+}}}} + i_{0,H^+/H_2} \cdot e^{\frac{E_{e.c,H^+/H_2} - E_{corr}}{\beta_{c,H^+/H_2}}}$$

$$-i_{0,Fe/Fe^{2+}} \cdot e^{\frac{E_{corr} - E_{e.a,Fe/Fe^{2+}}}{\beta_{a,Fe/Fe^{2+}}}} = \frac{i_{0,Fe^{3+}/Fe^{2+}} \cdot e^{\frac{E_{e.c,Fe^{3+}/Fe^{2+}} - E^*_{corr}}{\beta_{c,Fe/Fe^{2+}}}}}{1 + \frac{i_{0,Fe^{3+}/Fe^{2+}} \cdot e^{\frac{E_{e.c,Fe^{3+}/Fe^{2+}} - E^*_{corr}}{\beta_{c,Fe^{3+}/Fe^{2+}}}}}{i^*_{L,Fe^{3+}}}}$$

$$+ i_{0,H^+/H_2} \cdot e^{\frac{E_{e.c,H^+/H_2} - E^*_{corr}}{\beta_{c,H^+/H_2}}} - i_{0,Fe/Fe^{2+}} \cdot e^{\frac{E^*_{corr} - E_{e.a,Fe/Fe^{2+}}}{\beta_{a,Fe/Fe^{2+}}}} \tag{31}$$

$$\frac{i_{0,Fe^{3+}/Fe^{2+}} \cdot e^{\frac{E_{e.c,Fe^{3+}/Fe^{2+}} - E^*_{corr}}{\beta_{c,Fe^{3+}/Fe^{2+}}}}}{1 + \frac{i_{0,Fe^{3+}/Fe^{2+}} \cdot e^{\frac{E_{e.c,Fe^{3+}/Fe^{2+}} - E^*_{corr}}{\beta_{c,Fe^{3+}/Fe^{2+}}}}}{i^*_{L,Fe^{3+}}}} - \frac{i_{0,Fe^{3+}/Fe^{2+}} \cdot e^{\frac{E_{e.c,Fe^{3+}/Fe^{2+}} - E_{corr}}{\beta_{c,Fe^{3+}/Fe^{2+}}}}}{1 + \frac{i_{0,Fe^{3+}/Fe^{2+}} \cdot e^{\frac{E_{e.c,Fe^{3+}/Fe^{2+}} - E_{corr}}{\beta_{c,Fe^{3+}/Fe^{2+}}}}}{i_{L,Fe^{3+}}}}$$

$$+ \left(i_{0,H^+/H_2} \cdot e^{\frac{E_{e.c,H^+/H_2} - E^*_{corr}}{\beta_{c,H^+/H_2}}} - i_{0,H^+/H_2} \cdot e^{\frac{E_{e.c,H^+/H_2} - E_{corr}}{\beta_{c,H^+/H_2}}} \right)$$

$$- \left(i_{0,Fe/Fe^{2+}} \cdot e^{\frac{E^*_{corr} - E_{e.a,Fe/Fe^{2+}}}{\beta_{a,Fe/Fe^{2+}},}} - i_{0,Fe/Fe^{2+}} \cdot e^{\frac{E_{corr} - E_{e.a,Fe/Fe^{2+}}}{\beta_{a,Fe/Fe^{2+}}}} \right) = 0 \tag{32}$$

$$i_{0,Fe^{3+}/Fe^{2+}} \cdot e^{\frac{E_{e.c,Fe^{3+}/Fe^{2+}} - E_{corr}}{\beta_{c,Fe^{3+}/Fe^{2+}}}} \cdot \left(\frac{e^{\frac{E_{corr} - E^*_{corr}}{\beta_{c,Fe^{3+}/Fe^{2+}}}}}{1 + \frac{i_{0,Fe^{3+}/Fe^{2+}} \cdot e^{\frac{E_{e.c,Fe^{3+}/Fe^{2+}} - E^*_{corr}}{\beta_{c,Fe^{3+}/Fe^{2+}}}}}{i^*_{L,Fe^{3+}}}} - \frac{1}{1 + \frac{i_{0,Fe^{3+}/Fe^{2+}} \cdot e^{\frac{E_{e.c,Fe^{3+}/Fe^{2+}} - E_{corr}}{\beta_{c,Fe^{3+}/Fe^{2+}}}}}{i_{L,Fe^{3+}}}} \right)$$

$$+ i_{0,H^+/H_2} \cdot e^{\frac{E_{e.c,H^+/H_2} - E_{corr}}{\beta_{c,H^+/H_2}}} \cdot \left(e^{\frac{E_{corr} - E^*_{corr}}{\beta_{c,H^+/H_2}}} - 1 \right)$$

$$- i_{0,Fe/Fe^{2+}} \cdot e^{\frac{E_{corr} - E_{e.a,Fe/Fe^{2+}}}{\beta_{a,Fe/Fe^{2+}}}} \cdot \left(e^{\frac{E^*_{corr} - E_{corr}}{\beta_{a,Fe/Fe^{2+}}}} - 1 \right) = 0 \quad (33)$$

Eqn (33) shows that for iron in ferric solutions, the applied MF could change the reaction rate of ferric reduction by increasing the diffusion current density directly, and the reaction rates of proton reduction and iron dissolution indirectly through the change of OCP. It is not intended to solve eqn (32) analytically due to its complex form. The schematic diagram in Fig. 10 can be used for correlating the RCS for corrosion reactions under various combinations of cathodic and anodic reactions.

If there is only one cathodic reaction, $\Delta E_{corr,MF}$ can be expressed by eqn (34) for the fully MTS-controlled case and by eqn (35) for the fully ETS-controlled case. $\Delta E_{corr,MF}$ would lie between 0 and $\beta_a \ln\left(\frac{i^*_L}{i_L}\right)$ for the mixed control case by both ETS and MTS, eqn (36).

$$\Delta E_{corr,MF} = \beta_a \ln\left(\frac{i^*_L}{i_L}\right) \quad (34)$$

$$\Delta E_{corr,MF} = 0 \quad (35)$$

$$0 < \Delta E_{corr,MF} < \beta_a \ln\left(\frac{i^*_L}{i_L}\right) \quad (36)$$

The i_L under 0 T can be described by Fick's first law, as shown in eqn (37),[5,46] and the i^*_L under MF can be expressed by eqn (38).[35]

$$i_L = n \cdot F \cdot D \cdot c_0 / \delta \quad (37)$$

$$i^*_L = C_\mu \cdot B^{n_b} \cdot c_0^{n_c} \quad (38)$$

According to eqn (37) and (38), the ratio i^*_L/i_L can be expressed by eqn (39)

$$\frac{i^*_L}{i_L} = \frac{\delta \cdot C_\mu \cdot B^{n_b} \cdot c_0^{(n_{c-1})}}{n \cdot F \cdot D} \quad (39)$$

Combining eqn (34) and (39)

$$\Delta E_{corr,MF} = \beta_a \cdot \ln\left(\frac{\delta \cdot C_\mu \cdot B^{n_b} \cdot c_0^{(n_{c-1})}}{n \cdot F \cdot D}\right) \quad (40)$$

According to eqn (40), the change of $\Delta E_{corr,MF}$ with c_0 can be expressed by eqn (41) and the slopes are calculated with eqn (42):

$$\frac{\partial(\Delta E_{corr,MF})}{\partial c_0} = \beta_a \cdot (n_{c-1}) \cdot \frac{1}{c_0} \quad (41)$$

$$\frac{\partial^2(\Delta E_{corr,MF})}{\partial {c_0}^2} = -\beta_a \cdot (n_{c-1}) \cdot \frac{1}{{c_0}^2} \quad (42)$$

According to eqn (40), the change of $\Delta E_{corr,MF}$ with B can be expressed by eqn (43) and the slopes are calculated with eqn (44),

$$\frac{\partial(\Delta E_{corr,MF})}{\partial B} = \beta_a \cdot n_b \cdot \frac{1}{B} \quad (43)$$

$$\frac{\partial^2(\Delta E_{corr,MF})}{\partial B^2} = -\beta_a \cdot n_b \cdot \frac{1}{B^2} \quad (44)$$

According to Aaboubi *et al.*,[30] there are $n_c = 4/3$ and $n_b = 1/3$. Then, eqn 41–44 become eqn 45–48,

$$\frac{\partial(\Delta E_{corr,MF})}{\partial c_0} = \frac{1}{3} \cdot \beta_a \cdot \frac{1}{c_0} > 0 \quad (45)$$

$$\frac{\partial^2(\Delta E_{corr,MF})}{\partial {c_0}^2} = -\frac{1}{3} \cdot \beta_a \cdot \frac{1}{{c_0}^2} < 0 \quad (46)$$

$$\frac{\partial(\Delta E_{corr,MF})}{\partial B} = \frac{1}{3} \cdot \beta_a \cdot \frac{1}{B} > 0 \quad (47)$$

$$\frac{\partial^2(\Delta E_{corr,MF})}{\partial B^2} = -\frac{1}{3} \cdot \beta_a \cdot \frac{1}{B^2} < 0 \quad (48)$$

If MTS participates in the rate-controlling of the cathodic reaction, the value of $\Delta E_{corr,MF}$ would be positive, the values of $\frac{\partial(\Delta E_{corr,MF})}{\partial c_0}$ and $\frac{\partial(\Delta E_{corr,MF})}{\partial B}$ would be positive, while the values of $\frac{\partial^2(\Delta E_{corr,MF})}{\partial {c_0}^2}$ and $\frac{\partial^2(\Delta E_{corr,MF})}{\partial B^2}$ would be negative. These can be confirmed by the results in Fig. 1 for $\Delta E_{corr,MF}$, Fig. 2 for $\frac{\partial(\Delta E_{corr,MF})}{\partial B}$ and $\frac{\partial^2(\Delta E_{corr,MF})}{\partial B^2}$, and Fig. 3 for $\frac{\partial(\Delta E_{corr,MF})}{\partial c_0}$ and $\frac{\partial^2(\Delta E_{corr,MF})}{\partial {c_0}^2}$. The general trend predicted by the theoretical equations are consistent with the experimental results. It should be noted that the exact values calculated with the theoretical equations may not match the experimental data,

considering that the theoretical equations are obtained for fully MTS as RCS, while the actual case may not be true.

Based on these experimental observations and theoretical equations, it is proposed that if MF causes a positive shift in the OCP of a metal in a corrosive solution, MTS would participate in determining the rate of the cathodic reaction involved in corrosion at open circuit potential. This method may not be able to determine whether MTS is the sole RCS or one of the RCSs for the cathodic reaction. This can be addressed by the following method, based on the MF formulation that yields the current density and supporting experimental data.

4.2 Correlating magnetic field resulting in current density to RCS

The current density resulting from MF at potential E is shown in eqn (49), obtained by combining eqn (A13) and (18),

$$\Delta i_{MF}(E) = \frac{i_{0,Fe^{3+}/Fe^{2+}} \cdot e^{\frac{E_{e.c,Fe^{3+}/Fe^{2+}} - E}{\beta_{c,Fe^{3+}/Fe^{2+}}}}}{1 + \frac{i_{0,Fe^{3+}/Fe^{2+}} \cdot e^{\frac{E_{e.c,Fe^{3+}/Fe^{2+}} - E}{\beta_{c,Fe^{3+}/Fe^{2+}}}}}{i^{*}_{L,Fe^{3+}}}} - \frac{i_{0,Fe^{3+}/Fe^{2+}} \cdot e^{\frac{E_{e.c,Fe^{3+}/Fe^{2+}} - E}{\beta_{c,Fe^{3+}/Fe^{2+}}}}}{1 + \frac{i_{0,Fe^{3+}/Fe^{2+}} \cdot e^{\frac{E_{e.c,Fe^{3+}/Fe^{2+}} - E}{\beta_{c,Fe^{3+}/Fe^{2+}}}}}{i_{L,Fe^{3+}}}} \quad (49)$$

If ETS is the only RCS for ferric reduction at potential E, then

$$\Delta i_{MF}(E) = 0 \quad (50)$$

If MTS is the only RCS for the ferric reduction at potential E, then eqn (51) and (52) are valid,

$$\Delta i_{MF}(E) = i^{*}_{L,Fe^{3+}} - i_{L,Fe^{3+}} \quad (51)$$

$$\frac{\partial(\Delta i_{MF}(E))}{E} = 0 \quad (52)$$

Eqn (52) means that if the value of $\Delta i_{MF}(E)$ does not change with changing E in the potential range from $E_{PL,i}$ to $E_{PL,f}$, the RCS for the cathodic reduction rate of ferric ions can be thought to be fully controlled by MTS. The value of Δi_{MF} does not change with changing E in the potential range E_{PL} is shown in Fig. 5, combining with the values of $E_{PL,i}$, $E_{PL,f}$ and E_{PL}, as summarized in Table 1. According to eqn (51) and (52), the ferric reduction rate in the E_{PL} potential range is fully controlled by MTS. Δi_{MF} at potentials more positive than $E_{PL,i}$ is lower than that in $E_{PL,}$ as a result of the mixed control by both ETS and MTS, as indicated by the Δi_{MF} curve for the relatively high potentials in Fig. 10. The lower values of Δi_{MF} at potentials more negative than $E_{PL,f}$ than that in the E_{PL} potential range is thought to be related to the change of electrode surface condition resulting from fast proton reduction that has been observed during the potentiostatic polarization measurements. According to eqn (38), $i^{*}_{L,Fe^{3+}}$ would increase with increasing B and the concentration of ferric ions, there are,

$$\frac{\partial(\Delta i_{MF}(E))}{\partial B} > 0 \quad (53)$$

$$\frac{\partial(\Delta i_{MF}(E))}{\partial c_0} > 0 \quad (54)$$

The experimental results in Fig. 7 agree with eqn (53) and (54), where Δi_{MF} in the E_{PL} potential range increases with increasing B and c_0.

Based on the above electrochemical equations under MF and the experimental data, it is proposed that the RCSs for corrosion reaction with more than one cathodic reaction can be determined through the responses of OCP to the MF and the MF resulting current under potentiostatic polarization. A positive shift of OCP by the horizontal MF parallel to the vertically-placed iron working electrode can be used as the criterion for the contribution of MTS of ferric ions to the rate control. The cathodic reduction rate of ferric ions is fully controlled by MTS in the potential range where Δi_{MF} is independent of applied potential. The results of the weight loss tests in Fig. 8 show that the corrosion rate with 0.4 T MF is higher than that without MF for each concentration of ferric ions. Corrosion is accelerated by MF. The weight loss results are consistent with the theoretical analyses that MF would enhance the cathodic reaction with MTS participating in the cathodic reaction rate control, therefore accelerating the corrosion rate. The ratio $CR_{0.4T}/CR_{0T}$ was shown in Fig. 8b increasing with the increase of the ferric concentration, which follows the prediction by eqn (39) and the electrochemical data in Fig. 7, indicating that the enhancement factor by MF on cathodic diffusion rate is higher for a higher concentration of cathodic depolarizers.

Besides the direct effect of MF *via* its effect on mass transport or electrode kinetics, the change of the natural convection, such as solutional buoyancy or gas bubbling induced by MF, may also contribute to the response of the current density to the MF.[47–51]

Table 1 The potential range (E_{PL}) resulted from the $E_{PL,i}$ and $E_{PL,f}$ for Fe in 0.02, 0.05, 0.1 and 0.2 mol L^{-1} $Fe_2(SO_4)_3$ solutions

Electrode	$Fe_2(SO_4)_3$ x mol L^{-1}	$E_{PL,f}$ mV(SCE)	$E_{PL,i}$ mV(SCE)	E_{PL} mV(SCE)<
Fe	0.02	−619.8	−602.1	17.7
	0.05	−657.0	−606.5	50.5
	0.1	−598.9	−566.9	32.0
	0.2	−567.9	−543.6	24.3

Results in Fig. 8 have demonstrated that the effect of MF on proton reduction reaction, including gas bubbling in ferric solution, would be much less than that on ferric reduction. Some previous measurements of anodic or cathodic reactions under MF also indicate that the effect of solutional buoyancy would not play a significant role for iron in ferric solutions.[52,53] The changes of current density and OCP for iron in ferric solutions are thought to follow the proposed electrochemical kinetics equations, eqn 4–54.

5. Conclusions

In the present work, a series of electrochemical measurements and immersion tests with or without magnetic fields were designed to determine the RCS for the cathodic reaction on iron in ferric solution at potentials below the open circuit potential. Electrochemical kinetic equations under a magnetic field are proposed in the discussion to interpret the experimental results.

1. The magneto-electrochemical method can be used to determine the rate-controlling step for iron in ferric solutions, *i.e.*, by only the electron transfer step, or by only the mass transport step, or by both.

2. For iron in ferric solutions at open circuit potential, the rate-controlling step for cathodic reduction of ferric ions is a mixed type involving both the electron transfer step and the mass transport step, *i.e.*, not fully controlled by the mass transport step. There is a potential region where the rate for the cathodic reduction reaction of ferric ions is fully controlled by the mass transport step.

3. Open circuit potential shifts in the noble direction by the magnetic field as a result of the increase in the cathodic reduction rate of ferric ions, resulting from the magnetic field. The change of the open circuit potential and the increase of the cathodic current density due to the magnetic field increase with increasing B and the ferric concentration, while the increasing rate decreases with increasing B and the ferric concentration. The experimental observations are consistent with the results of the electrochemical kinetics equations.

4. A magnetic field increases the corrosion rate by accelerating the mass transport of ferric ions to the electrode surface, thereby accelerating cathodic reaction processes. The magnetic field-induced corrosion enhancement is greater at higher ferric concentrations.

Conflicts of interest

There are no conflicts to declare.

Abbreviations

B	Magnetic flux density, T
C_0	Ferric concentration in bulk solution, which is two times of the $Fe_2(SO_4)_3$ concentration, mol L^{-1}
CR	Corrosion rate, mg h^{-1} cm^{-2}
CR_{0T}	Corrosion rate under 0T, mg h^{-1} cm^{-2}
$CR_{0.4T}$	Corrosion rate under 0.4T magnetic field, mg h^{-1} cm^{-2}
E_{corr}	Open circuit potential values without magnetic field, mV;
E^*_{corr}	open circuit potential values with magnetic field, mV;
$E_{e.a}$	Equilibrium potential for the anodic dissolution reaction, mV;
$E_{e.c}$	Equilibrium potential for the cathodic reaction mV;
$i(E)$	Total current density, mA cm^{-2};
$i_{0,a}$	Exchange current density for the anodic dissolution reaction, mA cm^{-2};
$i_{0,c}$	Exchange current density for the cathodic reaction, mA cm^{-2};
$i_a(E)$	Total anodic current density at potential E, mA cm^{-2};
$i_c(E)$	Total cathodic current density at the potential of E, mA cm^{-2};
$i_{a,Fe/Fe^{2+}}(E)$	Anodic current density from dissolution of iron at potential E, mA cm^{-2};
i_{a1}	Anodic current density of anodic reaction 1 fully controlled by ETS under 0T, mA cm^{-2};
i^*_{a1}	Anodic current density of anodic reaction 1 fully controlled by ETS under magnetic field, mA cm^{-2};
i_{a2}	Anodic current density of anodic reaction 2 fully controlled by ETS under 0T, mA cm^{-2};
i^*_{a2}	Anodic current density of anodic reaction 2 fully controlled by ETS under magnetic field, mA cm^{-2};
i_{a3}	Anodic current density of anodic reaction 3 fully controlled by ETS under 0T, mA cm^{-2};
i^*_{a3}	Anodic current density of anodic reaction 3 fully controlled by ETS under magnetic field, mA cm^{-2};
$i_{c,Fe^{3+}/Fe^{2+}}(E)$	Cathodic current density from the reduction of Fe^{3+} at potential E, mA cm^{-2}
i_c	Total cathodic current density under 0T, mA cm^{-2};
i^*_c	Total cathodic current density under magnetic field, mA cm^{-2};
$i_{c,H^+/H_2}(E)$	Cathodic current density from the reduction of H^+ at potential E, mA cm^{-2};
$i_{c,O_2/\bar{O}H}(E)$	Cathodic current density from the reduction of O_2 at potential E, mA cm^{-2};
$i_{c,H_2O/H_2}(E)$	Cathodic current density from the reduction of H_2O at potential E, mA cm^{-2};
i_{c-1}	Cathodic current density of cathode reaction 1 fully controlled by ETS under 0T, mA cm^{-2}
i^*_{c-1}	Cathodic current density of cathode reaction 1 fully controlled by ETS under magnetic fieldmA cm^{-2};
i_{c-2}	Cathodic current density of cathode reaction 2 fully controlled by MTS under 0T, mA cm^{-2};
i^*_{c-2}	Cathodic current density of cathode reaction 2 fully controlled by MTS under magnetic field, mA cm^{-2};
i_{c+a1}	Total current density with anodic reaction 1 under 0T, mA cm^{-2};
i^*_{c+a1}	total current density with anodic reaction 1 under magnetic field, mA cm^{-2};
i_{c+a2}	Total current density with anodic reaction 2 under 0T, mA cm^{-2};

i^*_{c+a2}	total current density with anodic reaction 2 under magnetic field, mA cm^{-2};
i_{c+a3}	Total current density with anodic reaction 3 under 0T, mA cm^{-2};
i^*_{c+a3}	Total current density with anodic reaction 3 under magnetic field, mA cm^{-2};
i_L	Limiting current density for the cathodic reaction, mA cm^{-2}
m	The number of anodic reactions taking place on the electrode surface at a certain potential
n	The number of cathodic reactions taking place on the electrode surface at a certain potential;
n_b	Constant as exponent for B in eqn (38)
n_c	Constant as exponent for C_0 in eqn (38)
q	The charge of species in coulombs;
S	Surface area of the sample, cm^2;
t	Immersion time, h
W_0	Weight of the sample before the immersion test, mg;
W_1	Weight of the sample after the immersion test, mg;

Greek symbols

β_a	Tafel slope for the anodic dissolution reaction in ln scale, mV;
β_c	Tafel slope for the cathodic reaction in ln scale, mV;
δ	thickness of diffusion layer, m;
δ_{MF}	Factor for the magnetic field effect on reaction rate;
$\delta_{MF,a}$	Factor for the magnetic field effect on anodic reaction rate;
$\delta_{MF,c}$	Factor for the magnetic field effect on cathodic reaction rate;
Δi_{MF}	Current density resulting from the magnetic field, mA cm^{-2};

Data availability

All data generated or analyzed during this study are included in this article. The data underlying this article will be shared on reasonable request to the corresponding author.

Appendix

The total current density at potential E for corrodible materials immersed in corrosive solutions can be expressed by eqn (A1–A4).[44,54,55]

$$i(E) = i_c(E) - i_a(E) \quad (A1)$$

$$i_a(E) = \sum_m i_{a,m}(E) \quad (A2)$$

$$i_c(E) = \sum_n i_{c,n}(E) \quad (A3)$$

$$i(E) = \sum_n i_{c,n}(E) - \sum_m i_{a,m}(E) \quad (A4)$$

For iron in $Fe_2(SO_4)_3$ solutions, $i_c(E)$ can be written as eqn (A5).

$$i_c(E) = i_{c,Fe^{3+}/Fe^{2+}}(E) + i_{c,H^+/H_2}(E) + i_{c,O_2/OH^-}(E) + i_{c,H_2O/H_2}(E) \quad (A5)$$

The test $Fe_2(SO_4)_3$ solutions contain high concentrations of ferric ions and hydrogen ions as cathodic depolarizers; therefore, the reduction reactions of dissolved oxygen and water can be neglected in eqn (A5) if the potential is not far from the open circuit potential. Then, eqn (A5) becomes eqn (A6),

$$i_c(E) = i_{c,Fe^{3+}/Fe^{2+}}(E) + i_{c,H^+/H_2}(E) \quad (A6)$$

The anodic reaction for Fe in $Fe_2(SO_4)_3$ or H_2SO_4 solution at potentials not far from the open circuit potential is mainly from the active dissolution of iron, eqn (A7)

$$i_a(E) = i_{a,Fe/Fe^{2+}}(E) \quad (A7)$$

Thus, the $i(E)$ can be expressed by eqn (A8),

$$i(E) = [i_{c,Fe^{3+}/Fe^{2+}}(E) + i_{c,H^+/H_2}(E)] - i_{a,Fe/Fe^{2+}}(E) \quad (A8)$$

At E_{corr} under 0T, there is,

$$i(E_{corr}) = 0 \quad (A9)$$

Assuming that the anodic active dissolution of iron is determined by ETS, then

$$i_a = i_{0,Fe/Fe^{2+}} \cdot e^{\frac{E - E_{e,a,Fe/Fe^{2+}}}{\beta_{a,Fe/Fe^{2+}}}} \quad (A10)$$

Assuming that the reduction of hydrogen ions is controlled by ETS, which has been reported in the literature[1], then,

$$i_{c,H^+/H_2} = i_{0,H^+/H_2} \cdot e^{\frac{E_{e,c,H^+/H_2} - E}{\beta_{c,H^+/H_2}}} \quad (A11)$$

The cathodic current density for the reduction reaction of Fe^{3+} can be expressed by eqn (A12) by assuming that the reaction rate is controlled by a mixed type involving the MTS and ETS,

$$i_{c,Fe^{3+}/Fe^{2+}} = \frac{i_{0,Fe^{3+}/Fe^{2+}} \cdot e^{\frac{E_{e,c,Fe^{3+}/Fe^{2+}} - E}{\beta_{c,Fe^{3+}/Fe^{2+}}}}}{1 + \frac{i_{0,Fe^{3+}/Fe^{2+}} \cdot e^{\frac{E_{e,c,Fe^{3+}/Fe^{2+}} - E}{\beta_{c,Fe^{3+}/Fe^{2+}}}}}{i_{L,Fe^{3+}}}} \quad (A12)$$

Combining eqn (A10–A12), the $i(E)$ can be expressed by eqn (A13)

$$i(E) = \frac{i_{0,Fe^{3+}/Fe^{2+}} \cdot e^{\frac{E_{e.c,Fe^{3+}/Fe^{2+}} - E}{\beta_{c,Fe^{3+}/Fe^{2+}}}}}{1 + \frac{i_{0,Fe^{3+}/Fe^{2+}} \cdot e^{\frac{E_{e.c\ ,Fe^{3+}/Fe^{2+}} - E}{\beta_{c,Fe^{3+}/Fe^{2+}}}}}{i_{L,Fe^{3+}}}} + i_{0,H^+/H_2} \cdot e^{\frac{E_{e.c,H^+/H_2} - E}{\beta_{c,H^+/H_2}}} - i_{0,Fe/Fe^{2+}} \cdot e^{\frac{E - E_{e.a,Fe/Fe^{2+}}}{\beta_{a,Fe/Fe^{2+}}}} \quad (A13)$$

If $i_{L,Fe^{3+}} \ll i_{0,Fe^{3+}/Fe^{2+}} \cdot e^{\frac{E_{e.c,Fe^{3+}/Fe^{2+}} - E}{\beta_{c,Fe^{3+}/Fe^{2+}}}}$, *i.e.*, the reduction of ferric ions is fully controlled by MTS, eqn (A12) evolves to eqn (A14), and eqn (A13–A15),

$$i_{c,Fe^{3+}/Fe^{2+}} = i_{L,Fe^{3+}} \quad (A14)$$

$$i(E) = i_{L,Fe^{3+}} + i_{0,H^+/H_2} \cdot e^{\frac{E_{e.c,H^+/H_2} - E}{\beta_{c,H^+/H_2}}} - i_{0,Fe/Fe^{2+}} \cdot e^{\frac{E - E_{e.a,Fe/Fe^{2+}}}{\beta_{a,Fe/Fe^{2+}}}} \quad (A15)$$

If there is $i_{c,Fe^{3+}/Fe^{2+}} \gg i_{c,H^+/H_2}$ at potentials around the open circuit potential, eqn (A8) evolves to eqn (A16), and eqn (A13–A17),

$$i(E) = i_{c,Fe^{3+}/Fe^{2+}}(E) - i_{a,Fe/Fe^{2+}}(E) \quad (A16)$$

$$i(E) = \frac{i_{0,Fe^{3+}/Fe^{2+}} \cdot e^{\frac{E_{e.c,Fe^{3+}/Fe^{2+}} - E}{\beta_{c,Fe^{3+}/Fe^{2+}}}}}{1 + \frac{i_{0,Fe^{3+}/Fe^{2+}} \cdot e^{\frac{E_{e.c,Fe^{3+}/Fe^{2+}} - E}{\beta_{c,Fe^{3+}/Fe^{2+}}}}}{i_{L,Fe^{3+}}}} - i_{0,Fe/Fe^{2+}} \cdot e^{\frac{E - E_{e.a,Fe/Fe^{2+}}}{\beta_{a,Fe/Fe^{2+}}}} \quad (A17)$$

Based on eqn (A17), E_{corr} can be expressed by eqn (A18),

$$\frac{i_{0,Fe^{3+}/Fe^{2+}} \cdot e^{\frac{E_{e.c,Fe^{3+}/Fe^{2+}} - E_{corr}}{\beta_{c,Fe^{3+}/Fe^{2+}}}}}{1 + \frac{i_{0,Fe^{3+}/Fe^{2+}} \cdot e^{\frac{E_{e.c,Fe^{3+}/Fe^{2+}} - E_{corr}}{\beta_{c,Fe^{3+}/Fe^{2+}}}}}{i_{L,Fe^{3+}}}} = i_{0,Fe/Fe^{2+}} \cdot e^{\frac{E_{corr} - E_{e.a,Fe/Fe^{2+}}}{\beta_{a,Fe/Fe^{2+}}}} \quad (A18)$$

It is difficult to solve eqn (A18) analytically for E_{corr}. If the reduction of ferric ions is fully controlled by MTS, eqn (A18) comes eqn (A19)

$$E_{corr} = \beta_{a,Fe/Fe^{2+}} \cdot \ln(i_{L,Fe^{3+}}/i_{0,Fe/Fe^{2+}}) + E_{e,a,Fe/Fe^{2+}} \quad (A19)$$

Acknowledgements

This work has been supported by the Natural Science Foundation of China (No. 52271060).

References

1 P. Marcus, *Corrosion Mechanisms in Theory and Practise*, CRC press, Boca Raton, 3rd edn, 2012.
2 O. E. Barcia, O. R. Mattos, N. Pébère and B. Tribollet, *Electrochim. Acta*, 1996, **41**, 1385–1391.
3 D. Landolt, *Corrosion and Surface Chemistry of Metals*, EPEL press, Lausanne, 1st edn, 2007.
4 A. H. A. El-Geassy, *IOP Conf. Series: Mater. Sci. Eng.*, 2017, **229**, 012002.
5 A. J. Bard and L. R. Faulkner, *Electrochemical Methods Fundamentals and Applications*, John Wiley & Sons, New York, 2nd edn, 2001.
6 X. Tang, C. R. Ma, M. E. Orazem, C. You and Y. Li, *Electrochim. Acta*, 2020, **354**, 136631–136639.
7 C. F. Dong, A. Q. Fu, X. G. Li and Y. F. Cheng, *Electrochim. Acta*, 2008, **54**, 628–633.
8 M. C. Quevedo, G. Galicia, R. Mayen-Mondragon and J. G. Llongueras, *J. Mater. Res. Technol.*, 2018, **7**, 149–157.
9 V. Encinas-Sánchez, M. T. de Miguel, M. I. Lasanta, G. García-Martín and F. J. Pérez, *Sol. Energy Mater. Sol. Cells*, 2019, **191**, 157–163.
10 H. Schweickert, W. J. Lorenz and H. Friedburg, *J. Electrochem. Soc.*, 1980, **127**, 1693–1701.
11 C. Wang, S. H. Chen and X. L. Yu, *J. Electrochem. Soc.*, 1996, **143**, L283–L285.
12 C. Wang and S. H. Chen, *Electrochim. Acta*, 1998, **43**, 2225–2232.
13 Z. H. Lu, D. L. Huang, W. Yang and J. Congleton, *Corros. Sci.*, 2003, **45**, 2233–2249.
14 G. Yang, S. H. Chen, C. Wang and L. Li, *Electrochem. Commun.*, 2004, **6**, 643–647.
15 Z. P. Lu, D. L. Huang and W. Yang, *Corros. Sci.*, 2005, **47**, 1471–1492.
16 X. G. Yang, S. H. Chen, L. Li and C. Wang, *J. Electroanal. Chem.*, 2006, **586**, 173–179.
17 R. Sueptitz, J. Koza, M. Uhlemann, A. Gebert and L. Schultz, *Electrochim. Acta*, 2009, **54**, 2229–2233.
18 Z. P. Lu, T. Shoji and W. Yang, *Corros. Sci.*, 2010, **52**, 2680–2686.
19 B. Y. Yuan, J. L. Zhang, G. F. Gao, L. Li and C. Wang, *Electrochem. Commun.*, 2013, **27**, 116–119.
20 M. E. Ghabashy, G. H. Sedahmed and I. A. S. Mansour, *Br. Corros. J.*, 1982, **17**, 36–37.
21 M. A. Ghabashy, *Anti-Corros. Methods Mater.*, 1988, **35**, 12–13.
22 Z. P. Lu and J. M. Chen, *J. Chin. Soc. Corros. Prot.*, 1996, **16**, 37.
23 Z. P. Lu and J. M. Chen, *J. Chin. Soc. Corros. Prot.*, 1997, **17**, 203.
24 H. J. Li, F. Ning, H. Y. Dong, K. Zhang, Z. P. Lu, Y. J. Tang, S. W. Cai, T. M. Cui, J. R. Ma, X. H. Xu and S. C. Ling, *Corrosion*, 2020, **76**, 528–538.
25 H. Y. Dong, X. H. Xu, S. W. Cai, Y. J. Tang, Z. P. Lu, F. Ning, K. Zhang, J. R. Ma, T. M. Cui and Y. T. Zhang, *Corrosion*, 2021, **77**, 413–426.
26 H. J. Li, Q. Xiong, Z. P. Lu, J. J. Chen, Q. Xiao, X. K. Ru, S. C. Lin, J. R. Ma and Z. Chen, *Corros. Sci.*, 2017, **129**, 179–191.
27 Z. P. Lu, C. B. Huang, D. L. Huang and W. Yang, *Corros. Sci.*, 2006, **48**, 3049–3077.

28 G. Hind, J. M. D. Coey and M. E. G. Lyons, *Electrochem. Commun.*, 2001, **3**, 215–218.
29 T. Z. Fahidy, *J. Appl. Electrochem.*, 1983, **13**, 553–563.
30 O. Aaboubi, J. P. Chopart, J. Douglade, A. Olivier, C. Gabrielli and B. Tribollet, *J. Electrochem. Soc.*, 1990, **137**, 1796–1804.
31 R. A. Tacken and L. J. J. Janssen, *J. Appl. Electrochem.*, 1995, **25**, 1–5.
32 T. Z. Fahidy, *The Effect of Magnetic Fields on Electrochemical Processes: Modern Aspects of Electrochemistry*, Springer, US, 2002.
33 A. Ejaz, H. Y. Dong, X. H. Xu, T. M. Cui, Z. P. Lu, J. J. Chen, J. R. Ma and T. Shoji, *Corrosion*, 2022, **78**, 908–926.
34 H. N. Krogstad, R. Johnsen and M. Coey, *Corrosion*, 2018, **74**, 197–209.
35 L. M. A. Monzon and J. M. D. Coey, *Electrochem. Commun.*, 2014, **42**, 42–45.
36 E. J. Kelly, *J. Electrochem. Soc.*, 1976, **123**, C246.
37 S. Yamanaka, R. Aogaki, M. Yamato, E. Ito and I. Mogi, Tohoku University. Ser. A, Physics, *Chem. Metall.*, 1993, **38**, 399–405.
38 R. Aogaki, T. Negishi, M. Yamato, E. Ito and I. Mogi, *Physica B*, 1994, **201**, 611–615.
39 G. Hinds, F. E. Spada, J. M. D. Coey, T. R. N. Mhiochain and M. E. G. Lyons, *J. Phys. Chem. B*, 2001, **105**, 9487–9502.
40 D. Fernández and J. M. D. Coey, *Electrochem. Commun.*, 2009, **11**, 379–382.
41 Z. P. Lu and W. Yang, *Corros. Sci.*, 2008, **50**, 510–522.
42 Y. K. Sun, Y. H. Hu and X. H. Guan, *Environ. Sci. Technol.*, 2017, **51**, 3742–3750.
43 J. X. Li, H. J. Qin, W. X. Zhang, Z. Shi, D. Y. Zhao and X. H. Guan, *Sep. Purif. Technol.*, 2017, **176**, 40–47.
44 C. N. Cao, *Corrosion Electrochemistry Theory*, Chemical Industry Press, Beijing, 1985.
45 M. Stefanoni, U. Angst and B. Elsener, *Corrosion*, 2019, **75**, 737–744.
46 J. Li, B. Hurley and R. Buchheit, *Corrosion*, 2016, **72**, 1281–1291.
47 S. V. Gorobetsa, O. Y. Gorobetsb and S. A. Reshetnyakc, *J. Magn. Magn. Mater.*, 2004, **272–276**, 2408–2409.
48 O. Y. Gorobets, Y. I. Gorobets and V. P. Rospotniuk, *J. Appl. Phys.*, 2015, **118**, 073902.
49 M. Y. Ilchenko, O. Y. Gorobets, I. A. Bondar and A. M. Gaponov, *J. Magn. Magn. Mater.*, 2004, **322**, 2075–2080.
50 G. Mutschke, K. Tschulik, T. Weier, M. Uhlemann, A. Bund and J. Fröhlich, *Electrochim. Acta*, 2010, **55**, 9060–9066.
51 G. Mutschke, A. Hess, A. Bund and J. Fröhlich, *Electrochim. Acta*, 2010, **55**, 1543–1547.
52 H. Y. Dong, X. Li, X. Xu and Z. P. Lu, *RSC Adv.*, 2023, **13**, 8794–8802.
53 H. Y. Dong, H. J. Li, Y. Q. Tao, H. T. Chen, X. Li, J. Wang, Z. P. Lu, T. M. Cui, J. J. Chen, X. H. Xu and D. Pan, *RSC Adv.*, 2024, **14**, 1258–1266.
54 J. L. Hudson and T. T. Tsotsis, *Chem. Eng. Sci.*, 1994, **49**, 1493–1572.
55 F. Hilbert, Y. Miyoshi, G. Eichkorn and W. J. Lorenz, *J. Electrochem. Soc.*, 1971, **118**, 1919–1926.